

Validation study toward measuring the mechanical properties of blood clots using resonant acoustic spectroscopy with optical vibrometry

Gongting Wu^a, Alisa S. Wolberg^b, Amy L. Oldenburg^{a,c}

^aUniversity of North Carolina at Chapel Hill, Department of Physics and Astronomy, CB 3255, Chapel Hill, NC, USA 27599-3255;

^bUniversity of North Carolina at Chapel Hill, Department of Pathology and Laboratory Medicine, Chapel Hill, NC, USA 27599-7525;

^cUniversity of North Carolina at Chapel Hill, Biomedical Research Imaging Center, Chapel Hill, NC, USA 27599

ABSTRACT

Clot elastic modulus (CEM) has recently been shown to correlate with various hemostatic and thrombotic disorders and may be an important diagnostic parameter in cardiovascular diseases. Current methods of CEM measurement lack repeatability and require large sample volume. We present a novel method named resonant acoustic spectroscopy with optical vibrometry (RASOV) that has the potential to assess CEM with higher accuracy and speed, and lower sample volume. To validate RASOV, we measured the acoustic spectrum of agarose gel with varied concentrations in open-faced rectangular wells. Results showed a linear relationship between the natural resonant frequency and agarose content within a concentration range of 4 to 12 mg/mL. Furthermore, we observed that the resonant frequencies decrease with increasing transducer mass. As a highly accurate, resonance-based method, RASOV has great potential for biomechanical properties measurement, especially for human blood.

Keywords: Optical Vibrometry, Elasticity, Resonant Acoustic Spectroscopy, Resonance

1. INTRODUCTION

Cardiovascular disease (CVD) is the leading cause of death and disability in the world, causing over 17 million deaths in 2008.^[1] Methods for accurate assessment of CVD are needed for directing treatment. The stiffness of a blood clot, also known as clot elastic modulus (CEM), has been shown to correlate with various manifestations of CVD. For example, larger CEM was observed in patients with immunoglobulin G myeloma^[2] and patients with premature coronary artery disease.^[3] Altered fibrin clot structure was observed in patients with chronic obstructive pulmonary disease,^[4] patients with cryptogenic ischemic stroke,^[5] and patients with idiopathic venous thromboembolism.^[6] Thus, CEM may be an important diagnostic parameter in CVD.

Current methods and devices for assessing CEM include Thromboelastography (TEG),^{[7],[8]} Rotational thromboelastometry (ROTEM) and the Hemodyne.^[9] These methods are based upon measuring the ratio of stress to strain in the quasi-static regime. The biggest challenge for the quasi-static approach when measuring small (<1 cm³) and soft (<100 kPa) biosamples, such as blood clots, is the need for high measurement sensitivity of both force and displacement simultaneously.^[12] To achieve this typically requires using large, non-perturbative, stresses, and inevitably leads to poor accuracy, lack of repeatability, long measurement time and typically requires sample volumes (>100 μL). These drawbacks limit the popularity and availability of clinical CEM assessment devices.

To address these limitations, a novel technique called Resonant Acoustic Spectroscopy (RAS) was recently developed,^{[10],[11]} in which the elastic modulus is determined by measuring the sample's natural resonant frequency. Oldenburg and Boppart first demonstrated the relationship between acoustic resonances in tissues and elasticity.^[10] By employing embedded magnetic nanoparticles (MNPs) and modulating the tissue with a chirped-frequency (frequency-swept) stimulation, they successfully measured the mechanical resonant modes of cylindrical agarose phantoms with open sides, and calculated the Young's modulus from the resonant frequencies. Oldenburg *et al* further demonstrated the resonance modes of fibrin clots in an open-faced rectangular well by employing a metallic slab transducer. In that work, a high correlation between resonant frequency and fibrinogen content was found.^[11] These works show the potential of

RAS as a novel CEM assessment modality with high accuracy, fast speed, and small sample size requirement. In order to advance this technology, further validating studies are needed to investigate the effect of the transduction method on the measured acoustic resonances. In particular, we hypothesized that inertia from transducers of non-negligible weight will lower the observed resonance frequencies. In this paper, we measured the acoustic spectrum of agarose gel as a calibration material of similar elastic modulus as a blood clot, and compared the results using three different transducers: MNPs (negligible mass), a metallic slab (~2.2 mg) and a steel microbead (~4.1 mg). As we will show below, decreased resonant frequencies with increased transducer mass were observed.

2. MATERIALS AND METHODS

2.1 Sample preparation

Due to the similar stiffness between blood clots and agarose gel, and the simplicity of controlling the stiffness of agarose, we used water-based agarose gel as tissue phantoms to simulate the mechanical properties of human blood clots. Varying concentrations (3 – 12 mg/mL) of agarose (Type I-A, Low EEO, Sigma) solutions were mixed with ~0.7 mg/mL TiO₂ (powder, < 5 μm, Sigma), which were used to provide optical scattering in RASOV. For phantoms using embedded MNPs as the transducer, ~5 mg/mL Fe₃O₄ (nanopowder, < 50 nm, Sigma) were added to the solution. Mixtures were heated to above 85°C degree for 15 minutes and then gelled into open-faced rectangular wells for a total sample volume of 360 μL. Glass coverslips were used during the gelation process to flatten the surface and prevent dehydration. After curing for 24 hours, glass coverslips were removed from the sample and mechanical resonance spectra were collected.

2.2 RASOV system

Our RASOV system is coupled with a spectral-domain optical coherence tomography (OCT) system, identical to that used previously.^[10] A broadband Ti:Sapphire laser source centered at 800 nm with a bandwidth of ~125 nm (Griffin, Kapteyn-Murnane Labs, Boulder, Co) was used to provide an axial resolution of ~3 μm. A 30-mm-focal length objective lens was used to focus the laser beam to the sample, providing a lateral resolution of 12 μm. The average power incident on the sample was ~8 mW. The spectral interferograms were recorded by a line CCD camera (Dalsa Piranha 2) using 2048 pixels and a scan rate of 1, 2, or 5 kHz. An electromagnet is used to provide a gradient magnetic force on the transducer, which, in turn, transfers this force to the sample. The electromagnet is controlled by customized D/A convertor and a 288 W power amplifier (ATE 36-8M, Kepco), and can generate a peak magnetic field and gradient of 0.15 T and 15 T/m, respectively. A 625W water chiller (T255P, ThermoTek) was used to prevent overheating. A schematic of the experimental setup is shown in Figure 1. Our metallic slab is cut into a 2 mm x 2 mm x 0.025 mm (length x width x height) slab from an amorphous alloy sheet (Vacuumschmelze steel), and the mass of the slab is ~2.1 mg. The steel microbead we used is from McMaster, which has 1mm diameter and ~4.1 mg mass. The microwell resonator is made by customized 3D printing, the size of which is 6 mm x 6 mm x 10 mm.

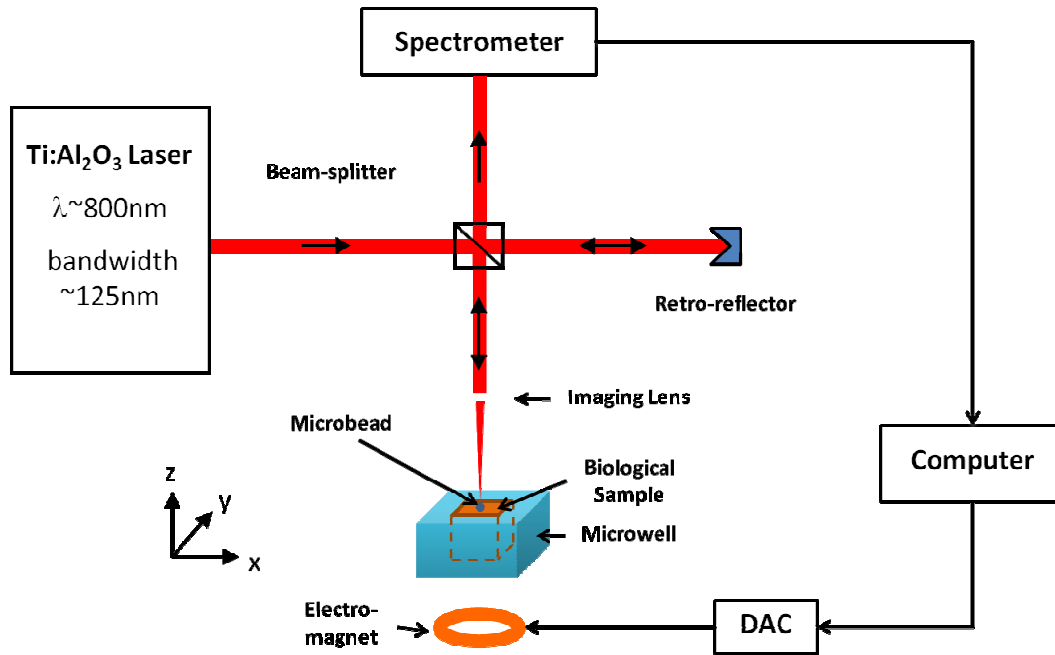


Figure 1. Schematic diagram of RASOV system. The laser beam is focused on the bead or the surface of the sample, tracking the simultaneous surface displacement when a chirped-frequency magnetic force is applied on the sample.

Though the general method for RAS is the same as described in previous work,^{[10],[11]} one major difference between this and the previous work is the introduction of a steel microbead as a microtransducer. The microbead is advantageous in that its optical backscattering is tunable by translating the beam across its surface, in order to achieve a signal within the dynamic range of the OCT system. Importantly, the microbead generates a vibration force that always points towards the magnet due to its spherically symmetric geometry. Furthermore, compared with MNPs, the microbead will not interfere with biochemical processes (such as the clotting process) as it does not change sample's chemical or mechanical properties.^[13] The only potential drawback of the microbead is its comparably larger mass, the impact of which is investigated here.

3. RESULTS AND DISCUSSION

3.1 Mechanical resonance spectrum

Magnetic nanoparticles (total mass <1.8 mg) that are embedded in the sample, a magnetic slab (~2.2 mg, Vacuumschmelze steel) wrapped with tape, and a steel microbead (~4.1mg, McMaster-Carr) were compared as transducers during our measurements. The laser beam was pointing at the center of the sample surface for agarose phantoms that had MNPs embedded. For RAS using a microtransducer, the laser beam was pointing at the center of the transducer which was placed at the center of the sample's top surface. An OCT image that scans across the agarose phantom with a microbead on top is shown in Figure 2.



Figure 2. OCT image of microbead on the top surface of an agarose phantom. Image dimensions are 7 mm × 2 mm (width × height).

When the measurement starts, a chirped-frequency signal is sent to magnet through the D/A convertor and amplified by the power supply, generating a varying frequency magnetic field. The sample will therefore be vibrated by the transducer while its surface displacement is simultaneously monitored by OCT. The mechanical spectrum is obtained as the vibration amplitude and phase lag versus driving frequency. The magnitude of the magnetic field is adjusted so that the sample only vibrates with amplitudes < 300 nm, corresponding to strains on the order of 0.003%. This ensures that our elasticity measurement is in the linear viscoelastic regime, where the displacement of the sample can be described as:

$$\Delta z(\omega) = \tilde{A}(\omega)e^{i\omega t} \quad (1)$$

and the vibration amplitude can be described by a complex Lorentzian function as follows:

$$\tilde{A}(\omega) = \frac{q}{\omega_n^2 - \omega^2 - i\omega\gamma_n} \quad (2)$$

where q is proportional to the driving force, ω_n is the resonant frequency of mode n and γ_n is the damping coefficient. By fitting the mechanical spectrum to this Lorentzian solution, the resonant frequency for different modes is then determined.

A representative example is shown in Figure 3. In this example, four resonant modes were observed. The fundamental mode ($n=0$) is around 284 Hz, with a strong peak amplitude and a characteristic phase lag shift from 0 (in-phase) at frequencies below the resonance, to π (out-of-phase) above the resonance. The phase lag shifts at the higher resonant modes become overlapped by one another, especially the third resonant mode and the fourth resonant mode. However, we were still able to determine the resonant frequency of these higher modes from fitting the amplitude spectrum. Also, we should note that a strong system background noise peak occurs at 60 Hz and its harmonics.

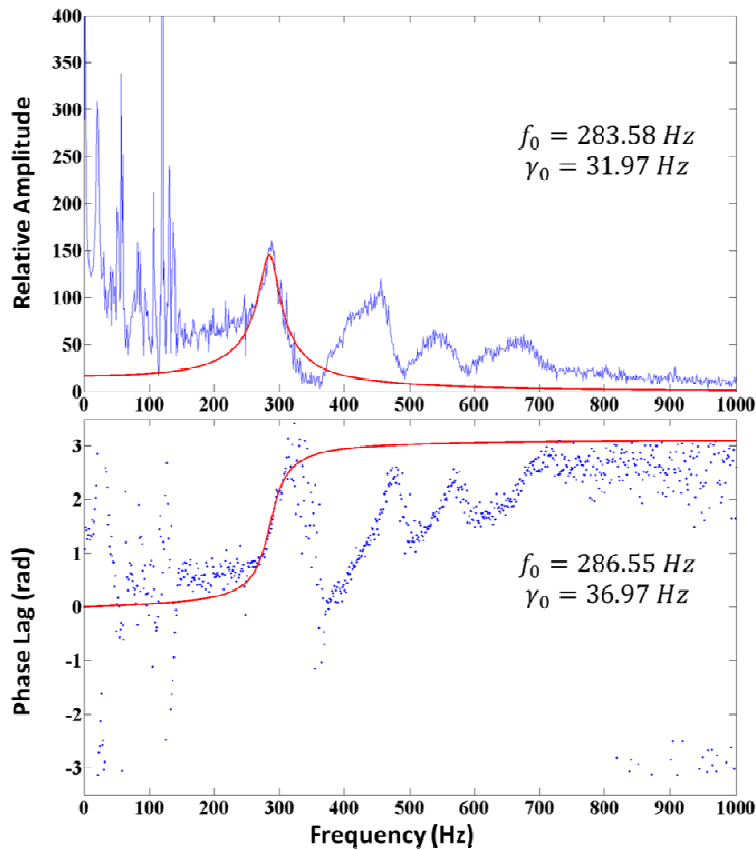


Figure 3. Acoustic spectrum of a 5.5 mg/mL agarose gel phantom. Least-squares fitting to the Lorentzian function was applied on both vibration amplitude and phase lag versus frequency to determine the natural resonant frequency.

3.2 Fundamental resonant frequency versus agarose concentration

Figure 4 shows the measured fundamental resonant frequency versus agarose content. A high correlation between fundamental resonant frequency and the agarose content was observed for all three transducers. Previous work by Oldenburg showed the relationship between the elastic modulus of agarose and concentration could be approximately described as a power law as follows:^[11]

$$E = 390 \times C^{2.09} \text{ Pa} \quad (3)$$

where E is the elastic modulus in Pa and C is the concentration of agarose gel in mg/mL. Also, the resonant frequency for each longitudinal mode n can be written as:

$$f_n = \frac{1}{\lambda_n} g \sqrt{\frac{E}{\rho}} \quad (4)$$

where λ_n is the wavelength of mode number n , E is the elastic modulus of the tissue, ρ is the mass density, and g is a geometrical factor that depends on the sample geometry, the boundary conditions, Poisson's ratio and the mode number n . From (3) and (4), we can write: $f_0 = bC^p$ where b and p are fitting parameters, and the fitting parameter $p=1.035$ is the power exponent relating concentration to resonant frequency. The fitting parameters for the microbead and metallic slab are close to that value. Fitting parameters are shown in Table 1.

At the same agarose concentration, decreased resonant frequency was observed with increasing transducer mass. This can be partly explained by using a spring model, where the gel can be treated as a spring (with non-negligible mass) with one end fixed, and the transducer is equivalent to a mass that is attached to the other end the spring. The resonant frequency of this spring system is inversely proportional to square root of the total mass of the system. For a nearly-incompressible biosample, vibration only occurs within the region near the top surface. Assuming the size of this region is $\sim 1/20^{\text{th}}$ of the sample volume, and the sample density equals the density of water ($1 \text{ mg}/\mu\text{L}$), the mass of this region is therefore 18 mg. Under this assumption, the resonant frequency measured by MNPs and a slab will be $\sim 11\%$ and $\sim 5\%$ respectively larger than the resonant frequency measured by a microbead. In comparison, the observed frequency increases were $\sim 70\%$ and $\sim 40\%$, respectively, and thus the expected frequency increase is much smaller than the observed frequency increase. A more complete model will be needed to quantitatively describe the effect of transducer's mass.

As we stated before, well-dispersed MNPs inside the agarose phantom may change the mechanical property of the sample. Our data show the resonant frequency measured by employing MNPs is much higher than that measured by using a microtransducer at the same agarose concentration, and that the difference is much larger than can easily be explained by the spring model. This suggests that the MNPs might stiffen the agarose sample.

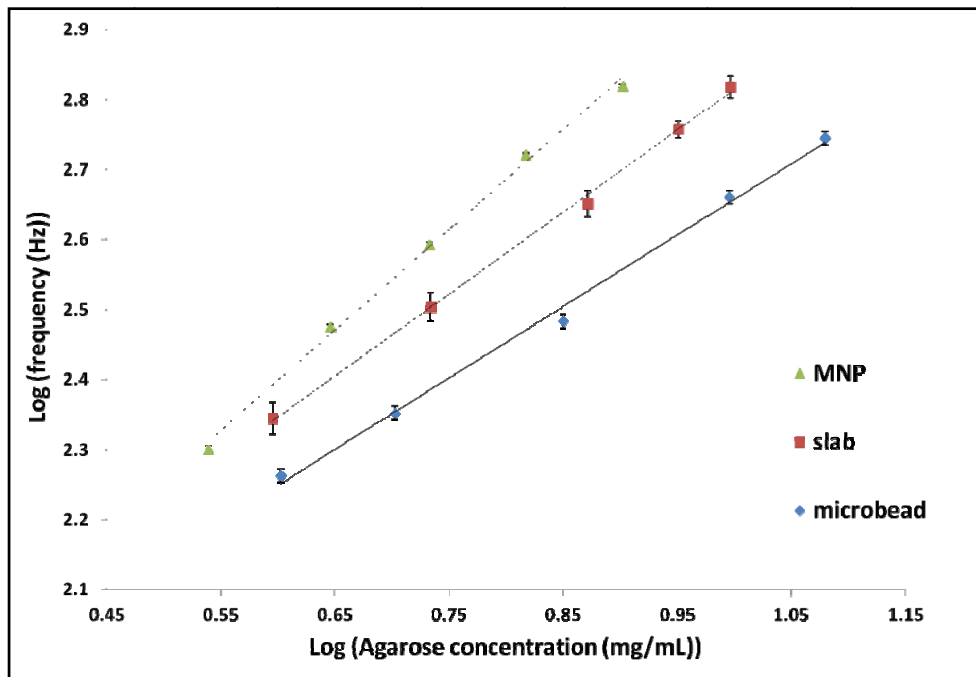


Figure 4. Concentration-dependent resonant frequencies of agarose gel using three different transducers and RASOV. A: Agarose gel with embedded magnetic nanoparticles. B: Magnetic slab on the phantom's top surface. C: Steel microbead on the phantom's top surface. Lines indicate best-fit curves with parameters reported in Table 1.

Table 1. Fitting parameters for resonant modes with three different transducers.

Fitting parameters:				
Transducer	Mass (mg)	p	b	R ²
MNPs	<1.0	1.43	34.8	0.9966
Slab	2.0	1.13	47.5	0.9984
Microbead	4.1	1.02	42.3	0.9958

4. CONCLUSION

This paper reports on the mechanical measurement of agarose gel in a closed microwell using RASOV. Acoustic spectra were obtained using three different types of transducers: Magnetic nanoparticles, a metallic slab, and a steel microbead. Results show a high correlation between the fundamental-mode frequency of agarose gel and the agarose concentration according to a power law. Furthermore, we show that weight of the transducer influences the resonant modes in the microwell, as the measured resonant frequencies increase with lower transducer weight. Current effort is underway to model the elastic response of this system when coupled to a microtransducer of non-negligible weight, in order to quantitatively extract Young's modulus from the resonance frequency measurement. These initial efforts constitute a baseline for calibrating the system response in the absence of such a model, which will be used in our future efforts to construct a clinical blood sampling instrument to measure CEM. Our works show a great potential of RASOV for clinical CEM assessment with high accuracy, fast speed and small sample volume.

5. ACKNOWLEDGEMENTS

We would like to thank Ava Pope, Karan Mohan and Raghav K. Chhetri for their laboratory assistance. This work is supported by the National Institutes of Health, National Heart, Blood, and Lung Institute 1R21HL109832 (Oldenburg, PI).

REFERENCES

- [1] World Health Organization, [Global Atlas on Cardiovascular Disease Prevention and Control], 3 (2011).
- [2] Carr, M.E., Zekert, S.L., "Abnormal clot retraction, altered fibrin structure, and normal platelet function in multiple myeloma," *Am. J. Physiol. Heart Circ. Physiol.*, 266, H1195-H1201 (1994).
- [3] Collett, J.P., Allali, Y., Lesty, C., Tanguy, M.L., Silvain, J., Ankri, A., Blanchet, B., Dumaine, R., Gianetti, J., Payot, L., Weisel, J.W., Montalescot, G., "Altered fibrin architecture is associated with hypofibrinolysis and premature coronary atherothrombosis," *Arterioscler. Thromb. Vasc. Biol.*, 26, 2567-2573 (2006).
- [4] Undas, A., Zawilska, K., Ciesla-Dul, M., Lehmann-Kopydlowska, A., Skubiszak, A., Ciepluch, K., Tracz, W., "Altered fibrin clot structure/function in patients with idiopathic venous thromboembolism and in their relatives," *Blood*, 114, 4272-4278 (2009).
- [5] Undas, A., Zaczmarek, P., Sladek, K., Stepień, E., Skucha, W., Rzeszutko, M., Gorkiewicz-Kot, I., Tracz, W., "Fibrin clot properties are altered in patients with chronic obstructive pulmonary disease," *Thromb. Haemost.*, 102, 1176-1182 (2009).
- [6] Undas, A., Podolec, P., Zawilska, K., Pieculewicz, M., Jedlinski, I., Stepień, E., Konarska-Kuszevska, E., Weglarz, P., Duszyńska, M., Hanschke, E., Przewlocki, T., Tracz, W., "Altered fibrin clot structure/function in patients with cryptogenic ischemic stroke," *Stroke*, 40, 1499-1501 (2009).
- [7] Spiess, B.D., Tuman, K.J., McCarthy, R.J., DeLaria, G.A., Schillo, R., Ivankovich, A.D., "Thrombelastography as an indicator of post-cardiopulmonary bypass coagulopathies," *J. Clin. Monit.*, 3, 25-30 (1987).
- [8] Donahue, S.M., Otto, C.M., "Thromboelastography: a tool for measuring hypercoagulability, hypocoagulability, and fibrinolysis," *J. Vet. Emerg. Crit. Care.*, 15, 9-16 (2005).
- [9] Carr, M.E., "Development of platelet contractile force as a research and clinical measure of platelet function," *Cell Biochem. Biophys.*, 38, 55-78 (2003).
- [10] Oldenburg, A.L., Boppart, S.A., "Resonant acoustic spectroscopy of soft tissues using embedded magnetomotive nanotransducers and optical coherence tomography," *Physics in Medicine and Biology*, 55(4), 1189-1201 (2010).
- [11] Oldenburg, A.L., Wu G., Spivak D., Tsui F., Wolberg A.S. and Fischer T., "Imaging and elastometry of blood clots using magnetomotive optical coherence tomography and labeled platelets," *IEEE Journal of Selected Topics in Quantum Electronics*, In Press (early online access).